# Synthesis and characterizations of three layered Zn$^{II}$, Cd$^{II}$ and Mn$^{II}$ coordination polymers with a flexible ligand [3-(2-pyridyl)-1-pyrazolyl] acetic acid

Lei Wang, Guang-Peng Jing, Pei Yang & Jing Chen

Taylor & Francis
Taylor & Francis Group

# Synthesis and characterizations of three layered Zn$^{II}$, Cd$^{II}$ and Mn$^{II}$ coordination polymers with a flexible ligand [3-(2-pyridyl)-1-pyrazolyl] acetic acid

LEI WANG, GUANG-PENG JING, PEI YANG and JING CHEN*

Tianjin Key Laboratory of Structure and Performance for Functional Molecules, MOE Key Laboratory of Inorganic-Organic Hybrid Functional Material Chemistry, College of Chemistry, Tianjin Normal University, Tianjin, People's Republic of China

Self-assembly of flexible [3-(2-pyridyl)-1-pyrazolyl] acetic acid (Hpypza) with ZnCl$_2$·4H$_2$O, CdCl$_2$·4H$_2$O, and Mn(OAc)$_2$·4H$_2$O affords three new coordination polymers [M(pypza)(HCOO)]$_n$ (M = Zn for 1; Cd for 2) and [Mn(pypza)(OAc)]$_n$ (3), which are significantly different from the previously reported complexes [Zn(pypza)Cl]$_2$, [Cd(pypza)Cl]$_n$, [Mn(pypza)Cl]$_2$, and [Mn(pypza)Cl]$_n$. These structural differences may be ascribed to the use of different solvents and anions.
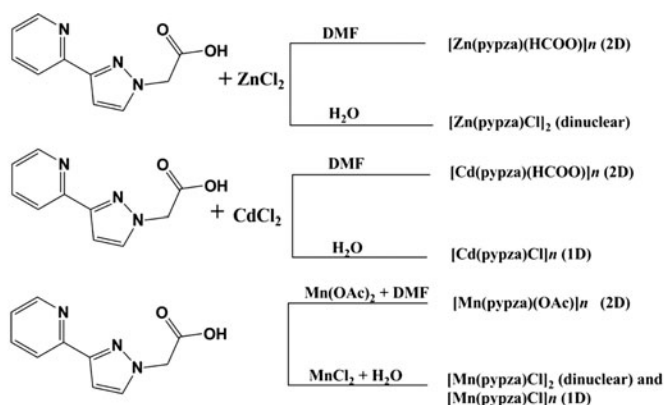
Self-assembly of flexible [3-(2-pyridyl)-1-pyrazolyl] acetic acid (Hpypza) with ZnCl$_2$·4H$_2$O, CdCl$_2$·4H$_2$O, and Mn(OAc)$_2$·4H$_2$O affords three new coordination polymers [M(pypza)(HCOO)]$_n$ (M = Zn for 1; Cd for 2) and [Mn(pypza)(OAc)]$_n$ (3), which are significantly different from the previously reported complexes [Zn(pypza)Cl]$_n$, [Cd(pypza)Cl]$_n$, [Mn(pypza)Cl]$_2$, and [Mn(pypza)Cl]$_n$. These structural differences may be ascribed to the use of different solvents and anions. Single-crystal X-ray diffraction analyses of these polymers indicate that **1** and **2** are isostructural with a 2-D coordination network via bridging pypza$^-$ and HCOO$^-$ resulting from the hydrolysis of DMF, and **3** also displays a 2-D network connected via pypza$^-$ and OAc$^-$. These complexes have been characterized by IR, microanalysis, and powder X-ray diffraction techniques. In addition, the solid

---

*Corresponding author. Email: hxxychj@mail.tjnu.edu.cn

fluorescence and thermal stability properties of **1–3** have also been investigated. Magnetic properties of the Mn$^{II}$ complex have also been measured.

## 1. Introduction

The design and synthesis of coordination polymers have received interest in recent years for their structural diversity and potential applications in catalysis, gas storage, optics, electronic conductivity, and magnetism [1–6]. Choice of organic building blocks plays an important role in such architectures [7–9]. Carboxylate and/or pyridyl-containing ligands constitute an important family of building blocks and have been selected to construct a variety of coordination architectures because of their robust and rich binding tendencies [10–13]. Pyrazole-based ligands have also been shown to form stable metal complexes due to elaboration of the pyrazole ring by various organic fragments [14–16]. Considering the above facts, we chose a pyrazole-derived ligand, [3-(2-pyridyl)-1-pyrazolyl] acetic acid (Hpypza), to construct coordination polymers with metal ions. As a pyrazole-derived ligand, Hpypza possesses pyridine, pyrazole, and carboxyl groups which should display diverse coordination, and the –CH$_2$– spacer between the pyrazole ring and carboxylate group offers flexible orientations of the carboxylate arm, favoring formation of various framework structures. Hpypza can be considered as an excellent and versatile building block, which has already been chosen to construct new crystalline materials by many scientists [17–19]. Among them, Yang *et al.* obtained [Zn(pypza)Cl]$_2$, [Cd(pypza)Cl]$_n$, [Mn(pypza)Cl]$_2$, and [Mn(pypza)Cl]$_n$ from assembly of Hpypza and ZnCl$_2$, CdCl$_2$ or MnCl$_2$, respectively, in water [20].

The type of solvent and anion influence the architectures of the coordination polymers [21–23]. With these considerations in mind, we aim to study the solvent and/or anion effect based on Hpypza. In this work, we chose [3-(2-pyridyl)-1-pyrazolyl] acetic acid as the ligand to assemble with ZnCl$_2$, CdCl$_2$, and Mn(OAc)$_2$ in DMF to afford three similar 2-D coordination layers [M(pypza)(HCOO)]$_n$ (M = Zn for **1**; Cd for **2**) and [Mn(pypza)(OAc)]$_n$ (**3**) under hydrothermal reaction conditions. The formate in **1** and **2** is *in situ* generated by hydrolysis of DMF. However, the HCOO$^-$ is not observed in **3** due to stronger binding ability of OAc$^-$ relative to HCOO$^-$. Complexes **1–3** have been characterized by IR, microanalysis, and powder X-ray diffraction (PXRD) techniques. Moreover, solid-state properties such as fluorescence, magnetic property, and thermal stability of all complexes have also been explored and discussed.

## 2. Experimental

### 2.1. *Materials and methods*

All reagents and solvents were commercially available and used as received. Carbon, hydrogen, and nitrogen elemental analyses were carried out with a CE-440 (Leemanlabs) analyzer. FTIR spectra (KBr pellets) were taken on an AVATAR-370 (Nicolet) spectrometer. PXRD patterns were recorded on a Rigaku D/Max-2500 diffractometer at 40 kV and

100 mA for a Cu-target tube ($\lambda = 1.5406$ Å). The calculated PXRD patterns were produced using the PowderCell program and single-crystal diffraction data. Thermogravimetric analysis experiments were performed on a TGA Q500 thermal analyzer from 25 to 600 °C (heating rate: 10 °C min$^{-1}$) under $N_2$. Fluorescence spectra of the solid samples were measured on a Cary Eclipse spectrofluorometer (Varian) at room temperature.

## 2.2. *Preparation of the complexes*

**2.2.1. Synthesis of [Zn(pypza)(HCOO)]$_n$ (1).** A mixture of $ZnCl_2 \cdot 4H_2O$ (20.8 mg, 0.1 mM) and Hpypza (10.2 mg, 0.05 mM) in DMF (10 mL) was sealed in a Teflon-lined stainless steel vessel (20 mL), heated to 120 °C for 48 h and then gradually cooled to room temperature at a rate of 5 °C h$^{-1}$. The resultant solution was filtered and left to stand at room temperature. After 20 days, the colorless block microcrystalline solid that formed was collected by filtration, washed with water, and ethanol, respectively, and dried in vacuo. Yield: 7.6 mg (49%, based on Hpypza). Anal. Calcd for $C_{11}H_9ZnN_3O_4$ (**1**): C, 42.27; H, 2.90; N, 13.44. Found: C, 42.58; H, 2.91; N, 13.49%. IR (KBr, cm$^{-1}$): 3413b, 1617vs 1604s, 1569w, 1444m, 1427m, 1369s, 1344m, 1244m, 1112w, 781m, 717w, 688m.

**2.2.2. Synthesis of [Cd(pypza)(HCOO)]$_n$ (2).** The same synthetic method as that for **1** was used except that $ZnCl_2 \cdot 4H_2O$ was replaced by $CdCl_2 \cdot 4H_2O$ (25.5 mg, 0.1 mM), affording colorless block single crystals of **2**. The solid was collected by filtration, washed with water followed by ethanol, and dried in vacuo. Yield: 5.2 mg (29%, based on Hpypza). Anal. Calcd for $C_{11}H_9CdN_3O_4$ (**2**): C, 36.74; H, 2.52; N, 11.68%. Found: C, 36.58; H, 2.59; N, 11.98%. IR (cm$^{-1}$): 3438b, 1640w, 1608s, 1551vs 1435s, 1369vs, 1190vs, 1104m, 1040vs 830m, 736s, 690s, 621s, 508m.

**2.2.3. Synthesis of [Mn(pypza)(OAc)]$_n$ (3).** The same synthetic method as that for **1** was used except that $ZnCl_2 \cdot 4H_2O$ was replaced by $Mn(OAc)_2 \cdot 4H_2O$ (24.5 mg, 0.1 mM), affording colorless block single crystals of **3**. The solid was collected by filtration, washed with water followed by ethanol, and dried in vacuo. Yield: 4.9 mg (31%, based on Hpypza). Anal. Calcd for $C_{12}H_{11}MnN_3O_4$ (**3**): C, 45.59; H, 3.51; N, 13.29. Found: C, 45.63; H, 3.59; N, 13.26%. IR (cm$^{-1}$): 3421b, 1595m, 1550m, 1439m, 1373m, 1313vs, 1243vs, 1163s, 1074s, 966m, 927m, 801w, 767vs, 717s, 665s, 621w, 591w, 496w. In addition, the same synthetic method as that for **3** was used except that HCOONa (6.8 mg, 0.1 mM) was added, affording the same block single crystals of **3**. Yield: 4.5 mg (29%, based on Hpypza).

## 2.3. *X-ray crystallography*

X-ray single-crystal diffraction data for all complexes were collected on a Bruker Apex II CCD diffractometer at ambient temperature with Mo Kα radiation ($\lambda = 0.71073$ Å). There was no evidence of crystal decay during data collection. Semi-empirical absorption corrections were applied (SADABS) and SAINT was used for integration of the diffraction profiles [24]. The structures were solved by direct methods using the SHELXS program of the SHELXTL package and refined with SHELXL [25, 26]. The final refinements were performed by full-matrix least-squares methods with anisotropic thermal parameters for all

Table 1.  Crystallographic data for **1–3**.

|  | **1** | **2** | **3** |
|---|---|---|---|
| Empirical formula | $C_{11}H_9ZnN_3O_4$ | $C_{11}H_9CdN_3O_4$ | $C_{12}H_{11}MnN_3O_4$ |
| Formula weight | 312.58 | 359.61 | 316.18 |
| Crystal system | Monoclinic | Monoclinic | Monoclinic |
| Space group | $P2_1/n$ | $P2_1/n$ | $P2_1/c$ |
| $a$/Å | 12.250(3) | 12.3366(11) | 9.6346(7) |
| $b$/Å | 7.532(2) | 7.8662(7) | 17.0994(13) |
| $c$/Å | 12.393(3) | 12.9261(12) | 8.0980(6) |
| $\alpha$/° | 90.00 | 90 | 90.00 |
| $\beta$/° | 92.656(4) | 93.1280(10) | 105.0130(10) |
| $\gamma$/° | 90.00 | 90 | 90.00 |
| $V$/Å$^3$ | 1142.2(5) | 1252.5(2) | 1288.57(17) |
| $Z$ | 4 | 4 | 4 |
| $F(0\,0\,0)$ | 632 | 704 | 644 |
| $D_c$/mg·m$^{-3}$ | 1.818 | 1.907 | 1.630 |
| $T$/K | 173(2) | 173(2) | 296(2) |
| $\mu$/mm$^{-1}$ | 2.165 | 1.757 | 1.041 |
| GOF | 1.088 | 1.040 | 1.027 |
| Reflections collected/unique | 5535/2000 | 6119/2209 | 6567/2279 |
| $R$(int) | 0.0289 | 0.0248 | 0.0229 |
| $R_1$, $wR_2$ [$I > 2\sigma(I)$] | 0.0264/0.0710 | 0.0188/0.0450 | 0.0289/0.0687 |
| $R_1$, $wR_2$ (all data) | 0.0291/0.0726 | 0.0212/0.0462 | 0.0424/0.0755 |

Table 2.  Selected bond lengths (Å) and angles (°) for **1–3**.

|  | **1** | **2** | **3** |
|---|---|---|---|
| M1–O1A | 2.1366(17) | 2.3498(16) | 2.1568(17) |
| M1–O2A | 2.2933(19) | 2.3778(17) | 2.525(2) |
| M1–O3 | 2.0727(17) | 2.2668(15) | 2.1180(17) |
| M1–O4B | 2.0486(18) | 2.2514(17) | 2.0828(17) |
| M1–N1 | 2.117(2) | 2.3247(19) | 2.266(2) |
| M1–N2 | 2.132(2) | 2.3177(18) | 2.2475(18) |
| O4B–M1–O3 | 91.27(7) | 98.96(6) | 89.50(7) |
| O4B–M1–O2A | 160.09(7) | 154.67(7) | 143.83(7) |
| O4B–M1–O1A | 100.54(7) | 99.07(6) | 88.95(7) |
| O4B–M1–N1 | 105.46(7) | 133.12(7) | 133.12(7) |
| O4B–M1–N2 | 89.21(7) | 87.41(6) | 99.40(7) |
| O3–M1–O2A | 93.37(7) | 154.67(7) | 96.61(7) |
| O3–M1–O1A | 95.84(7) | 97.45(6) | 103.10(7) |
| O3–M1–N1 | 93.72(7) | 93.39(6) | 88.06(7) |
| O3–M1–N2 | 76.90(8) | 163.48(6) | 159.59(7) |
| O2A–M1–O1A | 59.73(6) | 55.65(6) | 55.42(6) |
| O2A–M1–N1 | 93.55(7) | 99.07(7) | 83.05(7) |
| O2A–M1–N2 | 89.41(7) | 94.66(7) | 90.91(7) |
| O1A–M1–N1 | 152.04(7) | 153.10(6) | 136.99(7) |
| O1A–M1–N2 | 93.52(7) | 99.07(6) | 95.44(7) |
| N1–M1–N2 | 76.90(8) | 71.68(7) | 72.42(7) |

non-H atoms on $F^2$. Generally, C-bound hydrogen atoms were placed geometrically and refined as riding. Further crystallographic details are summarized in table 1 and selected bond lengths and angles are shown in table 2.

## 3. Results and discussion

### 3.1. *Description of crystal structures of 1 and 2*

Single-crystal X-ray diffraction analysis indicates that **1** and **2** are isostructural, and therefore, only the crystal structure of **1** will be described in detail. Notably, the attempt to assemble Hpypza with $M(OAc)_2/M(NO_3)_2$ (where M = Zn or Cd) in place of $MCl_2$ afford no X-ray diffraction suitable crystals. The asymmetric unit of **1** is composed of one $Zn^{II}$ center, one pypza$^-$, and one formate hydrolyzed from DMF. As depicted in figure 1(a), each distorted octahedral $Zn^{II}$ center is surrounded by three oxygens (O1A and O2A from the chelating carboxyl of pypza$^-$ and O4B from formate) and one nitrogen (N1 from the pyridyl ring of pypza$^-$) in the basal plane, and one nitrogen (N2 from the pyridyl ring of
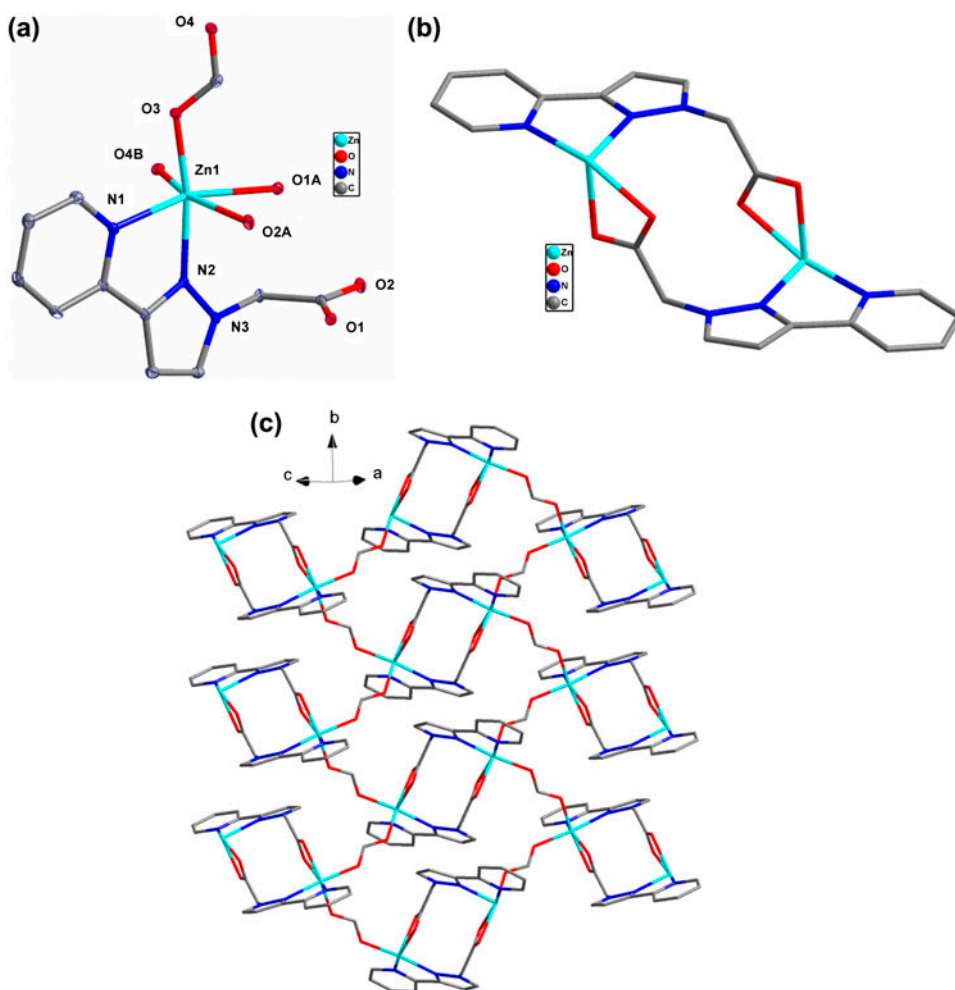


Figure 1. Crystal structure of **1**. (a) View of the asymmetric coordination unit and the coordination sphere of $Zn^{II}$ (thermal ellipsoids are drawn at the 30% probability level). (b) Dinuclear macrocyclic unit [$Zn_2(pypza)_2$]. (c) 2-D coordination network via the connection of pypza$^-$ and $HCOO^-$.

pypza$^-$) and one oxygen (O3 from formate) at the apical sites with the N2–Zn1–O3 angle of 170.4(1)°, displaying a distorted octahedral geometry. The Zn–O bond distances are from 2.049(2) to 2.293(2) Å and the Zn–N distances are 2.117(2) and 2.132(2) Å, all in a normal range observed in [Zn(pypza)Cl]$_2$ [20]. The bond distances of Zn–O4B (2.049(2) Å) and Zn–O3 (2.073(2) Å) to formate are significantly shorter than those of Zn–O$_{pypza}$−. The pypza$^-$ is a quadridentate chelating Zn$^{II}$ through the pyridine and pyrazole rings as well as the carboxyl of pypza$^-$. Two pypza$^-$ ligands bridge two Zn$^{II}$ ions to form a dinuclear macrocyclic [Zn$_2$(pypza)$_2$] with a Zn⋯Zn distance of 6.176(1) Å [figure 1(b)]. The [Zn$_2$(pypza)$_2$] dinuclear nodes are further connected via the bridging HCOO$^-$ with Zn⋯Zn distance of 5.859(1) Å to form a 2-D 4-connected **sql** coordination network, as shown in figure 1(c). Further analysis indicates that the adjacent 2-D layers stack parallel without any significant interactions (see Supporting Information). In addition, all coordinative bond distances in **2** also fall in the normal range compared to [Cd(pypza)(HCOO)]$_n$ [20], which are significantly longer than those in **1** because of the larger ionic radius of Cd$^{II}$ (table 2).

## 3.2. Description of crystal structure of 3

When ZnCl$_2$/CdCl$_2$ was replaced by Mn(OAc)$_2$·4H$_2$O, a similar 2-D coordination motif [Mn(pypza)(OAc)]$_n$ can be obtained for **3**. The reaction of Mn(NO$_3$)$_2$/MnCl$_2$ with Hpypza in the DMF does not afford expected crystalline materials. As shown in figure 2(a), each Mn$^{II}$ is surrounded by four oxygens from one chelating carboxyl group of pypza$^-$ (O1A and O2A) and two OAc$^-$ anions (O3 and O4B) and two nitrogens (N1 and N2) from the chelating pyridine and pyrazole rings of pypza$^-$, showing distorted octahedral geometry. The Mn–O bond distances are 2.083(2)–2.525(2) Å and the Mn–N bond distances are 2.248(2) and 2.266(2) Å, all in the normal range compared to [Mn(pypza)Cl]$_2$ [20] except Mn–O2 (2.525(2) Å). The Mn–O2 is significantly longer than other Mn–O bonds. Even so, the existence of Mn–O2 is reasonable because a much longer bond distance of Mn–O$_{carboxyl}$ (2.529(2) Å) has been reported in {[Mn$_3$(mip)$_2$(Hmip)$_2$(bpp)$_2$(H$_2$O)$_2$]·2H$_2$O}$_n$ (H$_2$mi*p* = 5-methylisophthalic acid and bp*p* = 1,3-di(4-pyridyl)propane) [27]. In **3**, pypza$^-$ adopts the quadridentate chelating coordination to connect adjacent Mn$^{II}$ centers forming a Mn$_2$(pypza)$_2$ dinuclear unit, with a Mn⋯Mn distance of 5.983(1) Å. Then with connection of OAc$^-$, a 2-D coordination network containing Mn$_2$(pypza)$_2$ dinuclear units is formed with Mn⋯Mn distance of 5.391(1) Å [figure 2(b)]. Furthermore, the adjacent 2-D layers are also stacking in a parallel fashion without any significant weak interactions (see Supporting Information).

## 3.3. Structural discussion of 1–3 and related complexes

Complexes **1**–**3** were prepared via self-assembly of Hpypza with ZnCl$_2$ (**1**), CdCl$_2$ (**2**), and Mn(OAc)$_2$ (**3**), respectively, affording similar 2-D coordination networks. The central Zn$^{II}$/ Cd$^{II}$/Mn$^{II}$ adopts the same octahedral geometries and pypza$^-$ is quadridentate chelating coordination in all complexes. The 2-D network of **3** is connected via pypza$^-$ and OAc$^-$, while the 2-D frameworks of **1** and **2** are connected by pypza$^-$ and HCOO$^-$ resulting from the hydrolysis of DMF. The hydrolysis of DMF led to unexpected products **1** and **2**. In fact, several examples of DMF hydrolysis in the construction of coordination compounds have been reported, in which it could hydrolyze in acidic solution under either normal or solvothermal conditions, giving formate or sometimes dimethylammonium [28–36]. Iversen *et al.*
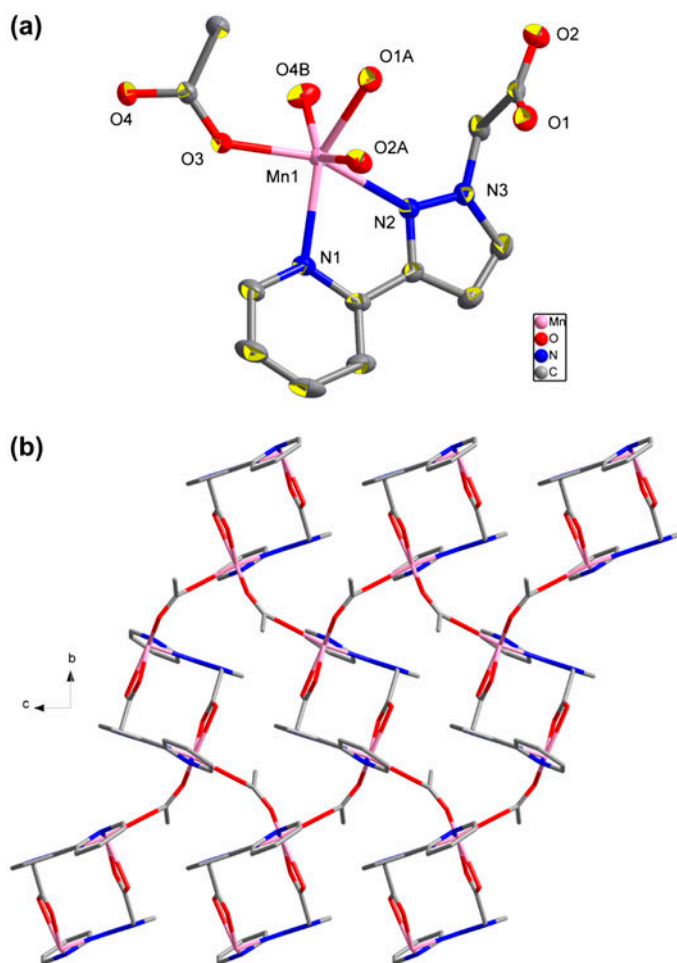
Figure 2. Crystal structure of **3**. (a) View of the asymmetric unit and the coordination environment of Mn[II] (thermal ellipsoids are drawn at the 30% probability level). (b) 2-D coordination network via the connection of pypza$^-$ and OAc$^-$.

reported the framework compound $(Me_2NH_2)[Zn(HCO_2)_3]$ in which both formate ligands and dimethylammonium cations arise from DMF hydrolysis [37]. For **3**, HCOO$^-$ is not observed in the structure, due to the stronger binding ability of OAc$^-$ relative to HCOO$^-$. In addition, we added HCOO$^-$ to reaction system of **3** affording the same block single crystals as **3**, which further confirm the stronger binding ability of OAc$^-$ relative to HCOO$^-$.

Hpypza has been investigated frequently to assemble with several metal salts previously [17–19]. Hpypza has different bridging coordination such as bidentate, tridentate, and quadridentate modes. The pypza$^-$ ligands are quadridentate chelating in **1–3**. Notably, Yang *et al.* used Hpypza to assemble with Zn[II], Cd[II], and Mn[II] under hydrothermal conditions, affording different complexes $[Zn(pypza)Cl]_2$ (dinuclear), $[Cd(pypza)Cl]_n$ (1-D), $[Mn(pypza)Cl]_2$ (dinuclear), and $[Mn(pypza)Cl]_n$ (1-D) in which Cl$^-$ coordinates to the metal centers in all complexes [20]. In $[Zn(pypza)Cl]_2$ and $[Mn(pypza)Cl]_2$, pypza$^-$ are chelating–bridging

metal ions through a pyridine N and a pyrazole N, and bridging two metal ions through a carboxyl O. In [Zn(pypza)Cl]$_2$ and [Mn(pypza)Cl]$_2$, the Zn–N$_{pyridine}$ bond length (2.178(3) Å) and the Mn–N$_{pyridine}$ bond length (2.283(3) Å) are slightly longer, while the Zn–N$_{pyrazole}$ bond length (2.029(4) Å) and the Mn–N$_{pyrazole}$ bond length (2.153(3) Å) are slightly shorter than those in **1** and **3**. The bond distances of Zn–O$_{carboxylate}$ (1.966(3) and 2.453(3) Å) and Mn–O$_{carboxylate}$ (2.099(3) and 2.264(3) Å) are similar to **1** and **3**. In [Cd(pypza)Cl]$_n$ and [Mn(pypza)Cl]$_n$, pypza$^-$ are quadridentate chelating as in **1–3**. The Cd–N bond lengths are 2.322 (5) and 2.346(5) Å and Cd–O are 2.326(4) and 2.418(5) Å, and the Mn–N bond lengths are from 2.217(6) to 2.271(6) Å and Mn–O are from 2.248(5) to 2.274(6) Å, all of which lie in the same range as **2** and **3**. Reaction of ZnCl$_2$/CdCl$_2$ with Hpypza in H$_2$O gives a dinuclear/ 1-D coordination network according to the literature, whereas 2-D layered structures [Zn(pypza)(HCOO)]$_n$/[Cd(pypza)(HCOO)]$_n$ are obtained in DMF with HCOO$^-$, resulting from hydrolysis of DMF. When Mn(OAc)$_2$ replaces MnCl$_2$ under the same hydrothermal condition in DMF, a higher-dimensional network of [Mn(pypza)(OAc)]$_n$ is obtained. The results demonstrate the influence of solvent and anion on the formation of coordination polymers of Zn$^{II}$, Cd$^{II}$, and Mn$^{II}$ based on Hpypza.

A variety of Zn$^{II}$, Cd$^{II}$, and Mn$^{II}$ coordination complexes have been reported based on the flexible carboxylate ligands, which simultaneously contain N-donor groups such as pyrazine, imidazole, triazole, and tetrazole. For example, Sun *et al.* [38] synthesized a series of coordination polymers based on 2-(1H-1,2,4-triazol-1-yl)acetic acid (HL), [Zn(L)$_2$(H$_2$O)$_2$]$_n$ and [Cd(L)$_2$]$_n$ are included. The Zn$^{II}$ and Cd$^{II}$ in the literature adopt the same octahedral geometries as **1** and **2**, respectively. With connection of carboxylate and triazole groups, Zn$^{II}$/Cd$^{II}$ are connected to afford (4,4)/(6,3)-connected 2-D coordination networks. Zhang *et al.* [39] have chosen a bifunctional ligand 1H-1,2,4-triazole-1-propionate (trzp$^-$) which has triazole and carboxylate groups, to assemble with Cd$^{II}$ affording a 2-D (4,4) coordination network {[Cd(trzp)$_2$(H$_2$O)]·2H$_2$O}$_n$. In this complex, the Cd$^{II}$ is pentagonal bipyramidal, different to the octahedral Cd$^{II}$ in **2**. In addition, Leciejewicz *et al.* [40] reported a mononuclear Mn$^{II}$ complex based on 2-pyrazinecarboxylic acid. In this complex, Mn$^{II}$ also adopts octahedral geometry, defined by pyrazine and carboxyl groups of ligand, and water ligands.

## 3.4. *IR, PXRD, fluorescence, TGA, and magnetic properties*

In IR spectra of **1–3**, the absence of the characteristic absorption at 1650–1700 cm$^{-1}$ indicates complete deprotonation of carboxyl. The phase purities of the complexes were also identified by PXRD patterns, which show essential similarity to the corresponding calculated patterns (see Supporting Information). It should be pointed out that the provided PXRD patterns are from several batches of crystals because of the low yield. Solid-state fluorescent properties of **1–3** were also measured at room temperature (see figure 3). Excitation of the microcrystalline samples leads to different fluorescent emissions showing emission maxima at 496 nm ($\lambda_{ex}$ = 290 nm) for **1**, 581 nm ($\lambda_{ex}$ = 337 nm) for **2**, and 496 nm ($\lambda_{ex}$ = 337 nm) for **3**. To explore the origin of these emission bands, the fluorescence spectra of Hpypza has also been measured (see Supporting Information), which show the emission peak at 375 nm ($\lambda_{ex}$ = 322 nm). In comparison to that of Hpypza, the significant redshift for the maximum emissions of **1–3** may be ascribed to ligand-centered transitions caused by metal-ligand coordinative interactions [41–45]. An obvious decrease of intensity is observed for these emission bands as compared to the free ligand, especially for Mn$^{II}$ complexes. TGA experiments were carried out to explore their thermal stability, which is an important
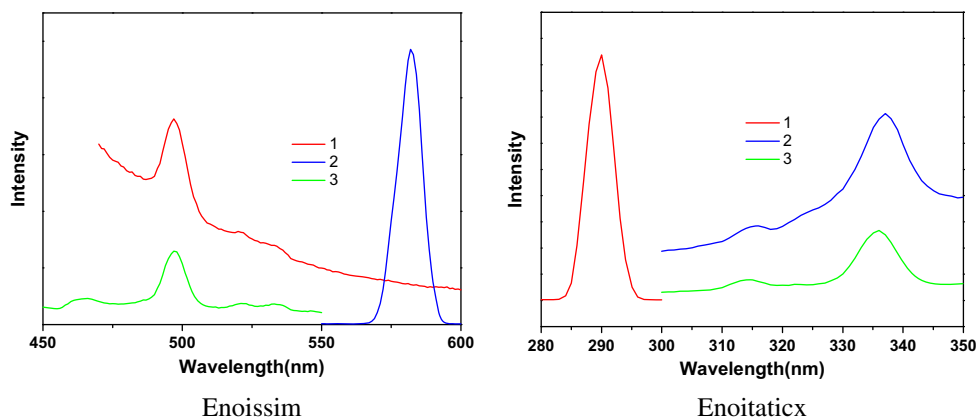
Enoissim                    Enoitaticx

Figure 3.   Solid-state fluorescent emission (left) and excitation (right) spectra of **1–3**.

parameter for coordination polymers (see figure 4). The TGA curves of **1–3** are similar due to their isostructural nature. The first weight loss of 0.7% for **1**, 1.8% for **2**, and 0.7% for **3**, from room temperature to 269, 213, and 306 °C, respectively, may be ascribed to water absorption for **1–3**. The remaining substances follow a series of sharp weight losses and hold a weight of 42.1%, 8.5%, and 39.3% of the total samples, respectively, until further heating to 600 °C. The material loses almost 92% for **2**, which can be ascribed to sublimation of CdO.

Magnetic susceptibility measurements for **3** were performed from 2 to 300 K with an applied field of 1000 Oe. The plot of $\chi_m T$ *versus T* is presented in figure 5. As can be seen from plots of experimental data, the experimental $\chi_m T$ value at 300 K is 4.55 cm$^3 \cdot$M$^{-1} \cdot$K, slightly larger than the spin-only value of 4.38 cm$^3 \cdot$M$^{-1} \cdot$K for one high-spin Mn(II) ($g = 2$, $S = 5/2$). The $\chi_m T$ value remains almost constant from 300 to 60 K,
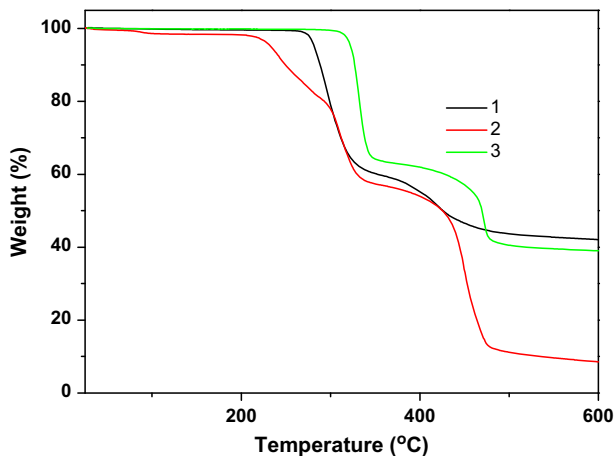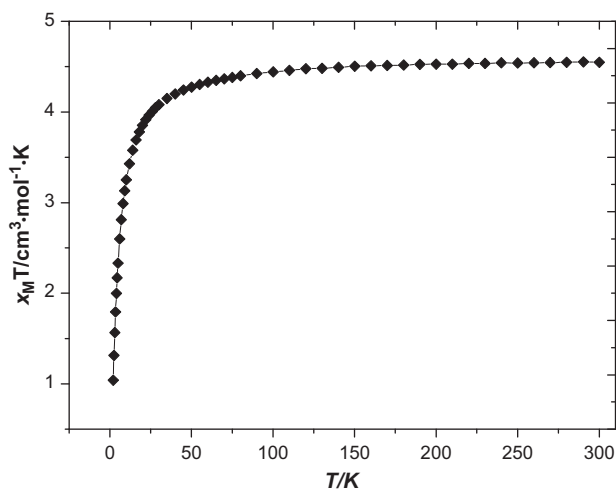


Figure 4.   TGA curves of **1–3**.

Figure 5.    The plot of $\chi_m T$ *vs.* $T$ for **3**.

and then decreases on further cooling, reaching a value of $1.05 \ \mathrm{cm^3 \cdot M^{-1} \cdot K}$ at 2 K. This behavior indicates a dominant antiferromagnetic interaction in **3**.

## 4.  Conclusion

Three new 2-D $Zn^{II}$, $Cd^{II}$, and $Mn^{II}$ coordination complexes based on Hpypza have been synthesized and characterized using different anions compared to the reported literature. The $HCOO^-$ ligands in **1** and **2** are *in situ* generated by hydrolysis of DMF, which is not observed in **3**. Our study shows that the change of solvents and anions can influence the subtle variables that lead to coordination polymers with different structures. Systematic exploration of effects on the construction of coordination polymers based on Hpypza is underway in our group.

## Supplementary material

Crystallographic data for the structural analysis have been deposited with the Cambridge Crystallographic Data Center, 989796–989798 for **1**–**3**. Copies of this information may be obtained free of charge at www.ccdc.cam.ac.uk/conts/retrieving.html [or from the Cambridge Crystallographic Data Center, 12 Union Road, Cambridge CB2 1EZ, UK]. Fax: C44 1223 336 066. Email: deposit@ccdc.cam.ac.uk.

## Funding

## Supplemental data

Supplemental data for this article can be accessed here [http://dx.doi.org/10.1080/00958972.2015.1016006].

## References

[1] S. Hu, K.H. He, M.H. Zeng, H.H. Zou, Y.M. Jiang. *Inorg. Chem.*, **47**, 5218 (2008).
[2] M. Du, C.P. Li, C.S. Liu, S.M. Fang. *Coord. Chem. Rev.*, **257**, 1282 (2013).
[3] W.T. Chen, S. Fukuzumi. *Inorg. Chem.*, **48**, 3800 (2009).
[4] M.D. Allendorf, C.A. Bauer, R.K. Bhakta, R.J.T. Houk. *Chem. Soc. Rev.*, **38**, 1330 (2009).
[5] M. Kurmoo. *Chem. Soc. Rev.*, **38**, 1353 (2009).
[6] M.N. Akhtar, Y.Z. Zheng, Y.H. Lan, V. Mereacre, C.E. Anson, A.K. Powell. *Inorg. Chem.*, **48**, 3502 (2009).
[7] L. Brammer. *Chem. Soc. Rev.*, **33**, 476 (2004).
[8] D.L. Long, R.J. Hill, A.J. Blake, N.R. Champness, P. Hubberstey, D.M. Proserpio, C. Wilson, M. Schröder. *Angew. Chem. Int. Ed.*, **43**, 1851 (2004).
[9] M. Du, Z.H. Zhang, L.F. Tang, X.G. Wang, X.J. Zhao, S.R. Batten. *Chem. Eur. J.*, **13**, 2578 (2007).
[10] X.L. Wang, C. Qin, E.B. Wang, L. Xu, Z.M. Su, C.W. Hu. *Angew. Chem. Int. Ed.*, 43, 5036 (2004).
[11] M. Du, X.J. Jiang, X.J. Zhao. *Inorg. Chem.*, **46**, 3984 (2007).
[12] A. Mishra, W. Wernsdorfer, K.A. Abboud, G. Christou. *J. Am. Chem. Soc.*, **126**, 15648 (2004).
[13] S.A. Barnett, N.R. Champness. *Coord. Chem. Rev.*, **246**, 145 (2003).
[14] S. Kitagawa, R. Kitaura, S. Noro. *Angew. Chem. Int. Ed.*, **43**, 2334 (2004).
[15] P.J. Steel. *Acc. Chem. Res.*, **38**, 243 (2005).
[16] O.R. Evans, W.B. Lin. *Acc. Chem. Res.*, **35**, 511 (2002).
[17] J.L. Du, X.L. Zhu, X.Y. Yang, T.L. Shen, L.J. Li. *J. Chem. Res.*, **36**, 680, (2012).
[18] Q.Y. Li, M.H. He, Z.D. Shen, G.W. Yang, Z.Y. Yuan. *Inorg. Chem. Commun.*, **20**, 214 (2012).
[19] H. Cai, Y. Guo, J.G. Li. *Inorg. Chem. Commun.*, **34**, 37 (2013).
[20] J. Yang, L. Shen, G.W. Yang, Q.Y. Li, L.L. Zhu, W. Shen, C. Ji, X.F. Shen. *Inorg. Chim. Acta*, **392**, 25 (2012).
[21] B. Wu, J. Yang, Y.Y. Liu, F.Y. Zhuge, N. Tang, X.J. Yang. *CrystEngComm*, **12**, 2755 (2010).
[22] M. Du, C.P. Li, J.H. Guo. *CrystEngComm*, **11**, 1536 (2009).
[23] A. Gutiérrez, M.F. Perpiñán, A.E. Sánchez, M.C. Torralba, M.R. Torres, M.P. Pardo. *Inorg. Chim. Acta*, **363**, 2443 (2010).
[24] Bruker A.X.S. *SAINT Software Reference Manual*, Madison, WI (1998).
[25] G.M. Sheldrick. *SHELXS-97: Program for the solution of crystal structures*, University of Göttingen, Germany (1997).
[26] G.M. Sheldrick. *SHELXL-97: Program for the refinement of crystal structures*, University of Göttingen, Germany (1997).
[27] L.F. Ma, L.Y. Wang, Y.Y. Wang, M. Du, J.G. Wang. *CrystEngComm*, **11**, 109 (2009).
[28] P. Yang, M.S. Wang, J.J. Shen, M.X. Li, Z.X. Wang, M. Shao, X. He. *Dalton Trans.*, **43**, 1460 (2014).
[29] J. Guo, D. Sun, L.L. Zhang, Q. Yang, X.L. Zhao, D.F. Sun. *Cryst. Growth Des.*, **12**, 5649 (2012).
[30] J.H. Liao, W.T. Chen, C.S. Tsai, C.C. Yang, C.C. Wang. *CrystEngComm*, **12**, 3033 (2010).
[31] G. Huang, P. Yang, N. Wang, J.Z. Wu, Y. Yu. *Inorg. Chim. Acta*, **384**, 333 (2012).
[32] S.M. Hawxwell, L. Brammer. *CrystEngComm*, **8**, 473 (2006).
[33] S.S. Chen, G.C. Lv, J. Fan, T.A. Okamura, M. Chen, W.Y. Sun. *Cryst. Growth Des.*, **11**, 1082 (2011).
[34] W. Chen, J.Y. Wang, C. Chen, Q. Yue, H.M. Yuan, J.S. Chen, S.N. Wang. *Inorg. Chem.*, **42**, 944 (2003).
[35] B. Zheng, J. Luo, F. Wang, Y. Peng, G. Li, Q. Huo, Y. Liu. *Cryst. Growth Des.*, **13**, 1033 (2013).
[36] D. Liu, Z. Chen, W. Huang, S. Qin, L. Jiang, S. Zhou, F. Liang. *Inorg. Chim. Acta*, **400**, 179 (2013).
[37] H.F. Clausen, R.D. Poulsen, A.D. Bond, M.A.S. Chevallier, B.B. Iversen. *J. Solid State Chem.*, **178**, 3342 (2005).
[38] X.Y. Zhou, Y.Q. Huang, W.Y. Sun. *Inorg. Chim. Acta*, **362**, 1399 (2009).
[39] Z. Zhang, D.F. Wu, K. Hu, Y.J. Shi, Z.L. Chen, F.P. Liang. *J. Coord. Chem.*, **66**, 2499 (2013).
[40] H. Ptasiewicz-Bąk, J. Leciejewicz, J. Zachara. *J. Coord. Chem.*, **36**, 317 (1995).
[41] M. Du, C.P. Li, X.J. Zhao, Q. Yu. *CrystEngComm*, **9**, 1011 (2007).
[42] M.L. Zhang, D.S. Li, J.J. Wang, F. Fu, M. Du, K. Zou, X.M. Gao. *Dalton Trans.*, 5355 (2009).
[43] Y.B. Dong, J.Y. Cheng, H.Y. Wang, R.Q. Huang, B. Tang. *Chem. Mater.*, **15**, 2593 (2003).
[44] L.L. Wen, D.B. Dang, C.Y. Duan, Y.Z. Li, Z.F. Tian, Q.J. Meng. *Inorg. Chem.*, **44**, 7161 (2005).
[45] D.S. Li, L. Tang, F. Fu, M. Du, J. Zhao, N. Wang, P. Zhang. *Inorg. Chem. Commun.*, **13**, 1126 (2010).